Design of a PV-Integrated EV Charging Station with Power Management Schemes

Anindya Bharatee
Department of Electrical Engineering
National Institute of Technology
Rourkela, India
bharatee.anindya@gmail.com

Pilla Sai Abhishek
Department of Electrical Engineering
National Institute of Technology
Rourkela, India
abhishekpilla9@gmail.com

Pravat Kumar Ray
Department of Electrical Engineering
National Institute of Technology
Rourkela, India
rayp@nitrkl.ac.in

***Abstract*—Here, the proposed work primarily focused on the planning of a grid-connected electric vehicle (EV) charging station integrated with a solar photovoltaic (PV) system. The foremost objective of the paper is to investigate the feasibility of utilizing renewable energy sources to charge EVs and to reduce the dependency on non-renewable energy sources. A multi-level constant current (MLCC) charging technique for EVs was implemented by considering the different states of charge (SOC) of EV batteries. Also, a constant DC bus voltage regulation-based power management scheme was implemented for optimal utilization of the sources and optimal sharing of active power. The control technique for the proposed PV-integrated EV charging station was verified through MATLAB/Simulink results and OPAL-RT experimental results.**

Keywords—renewable energy sources, photovoltaic, electric vehicle, power management schemes

I. INTRODUCTION

One of the major contributors to air pollution is the emissions from traditional fossil-fuel-powered vehicles. They have adverse impacts on the environment. Whereas, electric vehicles (EVs) have zero emission and may be powered using renewable energy, which makes them more sustainable and clean. Also, with the oil reserves being depleted and becoming harder to extract, there is a need to switch to some alternative energy to run the vehicles. Hence, nowadays EVs can be powered by renewable energy sources (RES) such as solar and wind, which also promotes energy independence. Also, EVs have lower maintenance and fuel costs compared to that traditional vehicles. Because of the increasing global awareness, the demand for the use of EVs is growing quickly. Hence, a large number of EVs are going to be operated in the near future, which may add huge stress to the existing electric grid for the charging process. To reduce the stress from the conventional grid, RES-based charging stations for EVs have been opted nowadays. This RES-based charging station keeps the surroundings clean and also saves the cost of transmission as the power is generated locally.

Many researchers are doing research on different EV charging techniques and power management strategies in charging stations. An overview of the on-board and off-board charging of EVs with one-way and two-way power flow schemes was presented in [1]. Normally unidirectional chargers provide simple interconnection topologies with limited hardware requirements and reduce the degradation of battery life. Whereas in the case of bidirectional charging, the battery injects the required power into the grid to provide adequate power stabilization. A DC bus signaling (DBS) based smart charging station was proposed in [2], where the voltage at the DC bus was variable and decided according to the Sun's insolation level. A multifunctional EV charging station was proposed in [3], where the system can run in both grid-integrated and stand-alone modes according to the availability of PV power. In [4], the authors presented an EV charging scheme based on inductive power transfer with a constant voltage/constant current (CV/CC) mode of charge with a wide range of load variation. An energy management system with PV power production forecasting capability was presented in [5] to control the optimal power flow between the grid, EV, and PV systems. Here, EV battery charging cost minimization is the main objective with reduced energy consumption from the grid. In [6], the authors designed a fast EV charging station with PV integration and storage devices. Here, the authors mainly focused to reduce the high energy demand from the conventional grid and to increase the profitability of the charging station. In [7], the authors proposed an approach to estimate the open-loop impact of plug-in-electric vehicle charging on a radial distribution system. This methodology utilized demographic data and travel surveys to predict the time and place of EV charging. An interval type-2 fuzzy logic-based power-sharing technique with EV charging was proposed in [8]. Here, a bidirectional power flow operation was developed for both grids to vehicle and vehicle to grid. In [9], a power management strategy with a hysteresis current controller for EV charging was proposed.

From the above literature, it is found that the integration of EV charging stations with PV systems can offer a renewable energy solution that not only reduces carbon emissions but also promotes sustainable transportation and achieves energy independence. Hence, this paper is based on the design of an EV charging station connected to a PV hybrid AC/DC microgrid. Here only the grid-to-vehicle mode of power flow is considered by using unidirectional buck converter interfacing. A multi-level constant current (MLCC) EV charging technique according to the available SOC level of batteries is proposed in this paper. Additionally, a power management scheme based on DC bus voltage is proposed to maintain a constant DC link voltage and provide uninterrupted charging of EVs during variable load and PV generation.

This paper is structured as follows: the detailed structural design of the proposed EV charging station is described in Section II followed by the control techniques of different converters in Section III. In Section IV simulation results are discussed and real-time OPAL-RT results with explanations are given in Section V. Lastly, concluding remarks with the future field of application are given in Section VI.

II. STRUCTURAL DESIGN OF PROPOSED EV CHARGING STATION

The complete structure of the planned EV charging station is shown in Fig. 1. It consists of a PV array, utility grid, electric vehicle, and DC loads. A DC/DC boost converter is used for the interfacing of the PV array with the common DC bus. The switching control of this boost converter is done by implementing maximum power point tracking (MPPT)

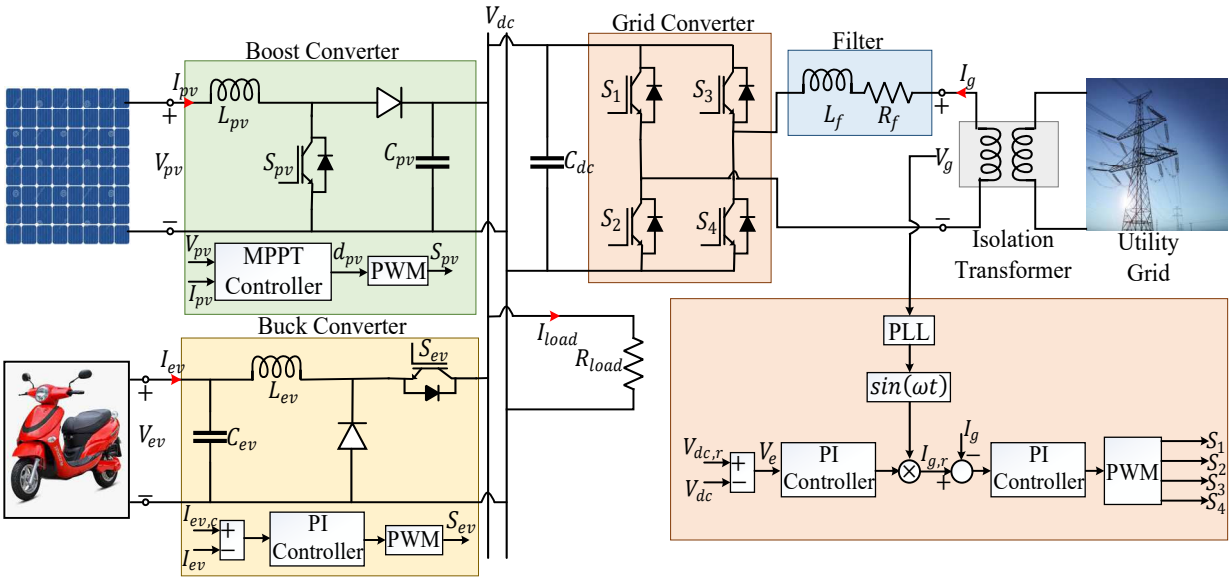

Fig. 1. Complete architecture with control techniques of the proposed EV charging station.

technique for extraction of the maximum possible PV power. Then, the electric vehicle is connected to the microgrid by using a buck converter. In this paper, the EV is represented as a battery unit in the system. A bidirectional AC/DC converter is used with the connected grid to provide the provision of a two-way power flow in order to maintain the proper power balance in the system.

III. Control Structure of Proposed EV Charging Station

The amount of power produced from PV is not constant every time because of the intermittent nature of the environment. Hence, according to the available PV power, a power balance should be maintained in the system for a safe and reliable operation. Hence, the power balance equation can be given as

$$P_{pv} + P_g = P_{load} + P_{ev} \tag{1}$$

P_{pv}, P_g, P_{load}, and P_{ev} are the power of PV, grid, load, and EV respectively. Depending on (1), two modes of operation are defined in this paper.

1. Sufficient power ($P_{pv} > P_{load} + P_{ev}$): In this working mode, the power produced from PV is enough to supply the DC load and EV charging. The additional available power from PV is absorbed by the grid.
2. Insufficient Power ($P_{pv} < P_{load} + P_{ev}$) : In this operation, the PV power alone is not enough to meet the load demand and EV charging. Hence, the extra power required in the microgrid is supplied by the grid unit.

A. Control of AC/DC Converter

This is a bidirectional AC/DC converter mainly used for interfacing the grid with a microgrid system and to maintain the constant voltage at a common DC link. During sufficient power mode, it works as a DC/AC converter and during insufficient power mode, it works as an AC/DC converter. For the switching control of this converter, the control technique used is based on DC bus voltage.

$$V_e = V_{dc,r} - V_{dc} \tag{2}$$

V_{dc} and $V_{dc,r}$ are the actual and reference voltage at the DC bus, and the error voltage at the DC bus is noted as V_e. The minimum reference DC bus voltage can be calculated by using (3) according to the grid voltage [10]. In this paper, the single-phase grid is having $230V$, hence the DC bus reference voltage is chosen as $400V$.

$$V_{dc,r} = \frac{2\sqrt{2}V_g}{\sqrt{3}} \tag{3}$$

$$I_{g,r} = V_e\left(K_p + \frac{K_i}{s}\right) \times \sin(\omega t) \tag{4}$$

The reference grid current ($I_{g,r}$) is generated in (4) by using a voltage controller with the voltage deviation at the DC bus. K_p and K_i are the proportional and integral coefficients of the voltage controller. A phase-locked loop (PLL) is implemented to compute the grid voltage template ($\sin(\omega t)$) and accordingly, the current reference will be estimated. ω is the angular frequency of the grid. Then, the generated reference current and actual current of the utility grid are compared, and output is given to a PI-based current controller as shown in Fig. 1. The switching signals for S_1 to S_4 are produced by using a PWM generator.

The minimum value of the DC link capacitor (C_{dc}) can be calculated as [11]

$$C_{dc} = \frac{3V\alpha It}{\frac{1}{2}\left[{V_{dc}}^2 - {V_{dc,min}}^2\right]} \tag{5}$$

Here, V is the voltage (phase), I is the current (phase), α is the factor for overload, and $V_{dc,min}$ is the minimum permissible DC bus voltage. The minimum filter inductance (L_f) value can be estimated as

$$L_f = \frac{\sqrt{3}mV_{dc}}{12\alpha f_{sw}\Delta i} \tag{6}$$

In (6), $m, \alpha, \Delta i,$ and f_{sw} are the modulation index, overloading factor, current ripple, and switching frequency of AC/DC converter, respectively [11].

B. Control of DC/DC Boost Converter

A boost converter as presented in Fig. 1 is utilized to boost the PV voltage level which is then fed to the DC bus. A perturb and observe (P&O) MPPT algorithm is implemented in this

paper for tracking of the maximum PV power. The MPPT is taking the PV voltage (V_{pv}) and PV current (I_{pv}) as input. The duty cycle (d_{pv}) from the MPPT is given to the PWM generator to generate the switching pulses for S_{pv}. The boosting operation of the converter will be decided by the voltage of PV and DC bus voltage as follows.

$$V_{dc} = \frac{V_{pv}}{1-d_{ev}} \tag{7}$$

C. Control of DC/DC Buck Converter

Different types of charging techniques for EV batteries are discussed in [12] such as i) constant voltage (CV), ii) constant power (CP), iii) constant current (CC), iv) trickle current (TC), v) taper and floating charging, etc. Normally, the constant current charging method is used widely for EV charging systems. In this paper, a modified CC charging technique is utilized that is multi-level constant current (MLCC) charging. Here, the charging current for EV batteries varies with the SOC level of the EVs. The running SOC level of the batteries can be calculated by applying the following equation.

$$SOC = SOC_{init} - \frac{1}{3600C}\int I_{ev}dt \tag{8}$$

In (8), SOC_{init}, C, and I_{ev} are the initial SOC value of EV, nominal capacity of batteries, and the EV current respectively. The initial SOC value of EV can be found from the open circuit voltage of the EV batteries.

The MLCC charging method continuously monitors the SOC levels and generates the reference EV charging current ($I_{ev,c}$). The minimum and maximum SOC limits are 20% and 80% respectively. When the SOC of batteries is less, the charging current will be more and vice versa. The EV charging current is a maximum that is $9A$ when the SOC is less than the lower limit of 20%. Then from 20% to 50% of SOC, the charging current is set to $7A$, and from 50% to 80%, it is set as $5A$. After 80% of charging, the control technique stops the EV charging process to avoid overcharging the EV batteries.

IV. Simulation Results and Discussion

The proposed EV charging technique is verified by the results obtained from MATLAB simulations. In Table I, the designed parameters of the proposed system are given.

TABLE I. System Design Parameters

PV Parameters (for a single array)	
Maximum voltage (V_{mp})	$29V$
Open circuit voltage (V_{oc})	$36.3V$
Maximum current (I_{mp})	$7.35A$
Short circuit current (I_{sc})	$7.84A$
EV Battery	
Nominal voltage	$12V$
Number of batteries	16
Initial SOC	35%
Grid voltage, frequency	$230V, 50Hz$
DC bus voltage	$400V$

During all operating conditions, the losses in power because of the passive elements present in the system are not considered for the simulation study.

A. Change in PV Generation

Initially, the irradiance is $1000\,W/m^2$ from $0-3s$ and then it is decreased to $500\,W/m^2$ from $3-6s$. The load requirement and EV charging power remain constant throughout this operation. From $0-3s$, PV generation is $1450W$ and EV is charging with a constant power of $1350W$. A sufficient amount of PV power is produced to meet the charging of EVs. Then, the grid is supplying the extra power of $1100W$ to the DC load as presented in Fig. 2. At $3s$, PV generation is reduced to $750W$, but EV is taking constant power for charging purposes. The additional EV charging power is delivered by the utility grid, hence grid power is increased to $1850W$. During these changes of power, the voltage at the DC link is maintained at a constant value of $400V$ as presented in Fig. 3. Maintenance of constant DC bus voltage regardless of any changes in the microgrid is one of the prime functional intentions in a power management system. During this operating mode, EV is in charging mode. As shown in Fig. 4, the SOC of EV is increasing gradually with time.

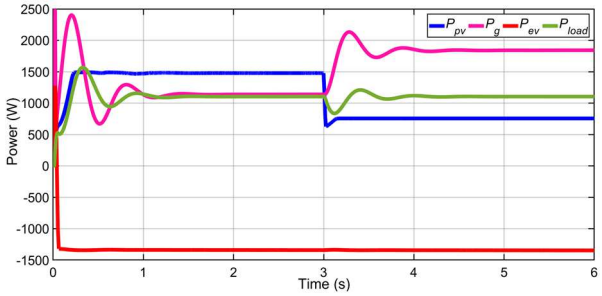

Fig. 2. Different power plots during PV power variation.

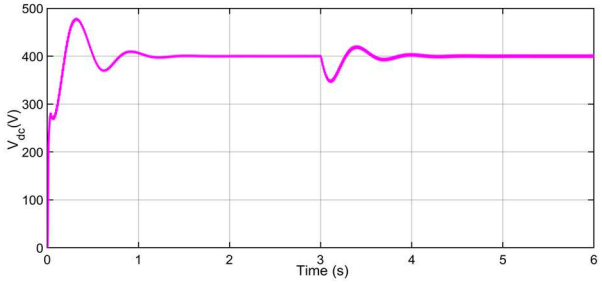

Fig. 3. DC bus voltage during PV power variation.

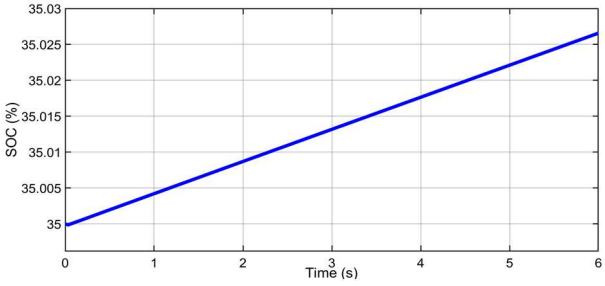

Fig. 4. Change in SOC of EV during charging condition.

B. Change in Load

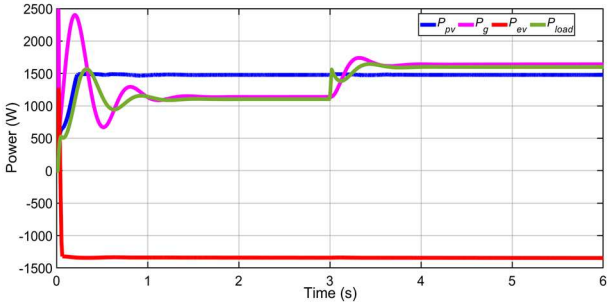

Fig. 5. Different power plots during the change in load demand.

During this operating condition, PV generation and EV charging power are constant. The load requirement is $1100W$ initially from $0-3s$. At $3s$, the load is increased to $1650W$. The additional power demanded by the load is met by the grid. Hence, the amount of power drawn from the connected grid is also increased as displayed in Fig. 5.

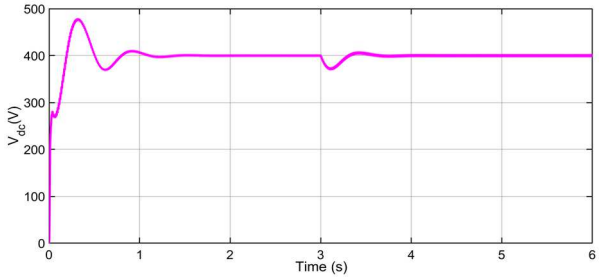

Fig. 6. DC bus voltage during the change in load.

The voltage at DC link is kept constant during the change in load condition. At $3s$, there is a deviation in the DC bus voltage, but it regained the $400V$ after $0.2s$ as shown in Fig. 6. In this mode, the utility grid is providing power to the microgrid, hence the voltage and current at the grid side are operated at unity power factor (UPF) as given in Fig. 7. This will improve the quality of power delivered to the consumers.

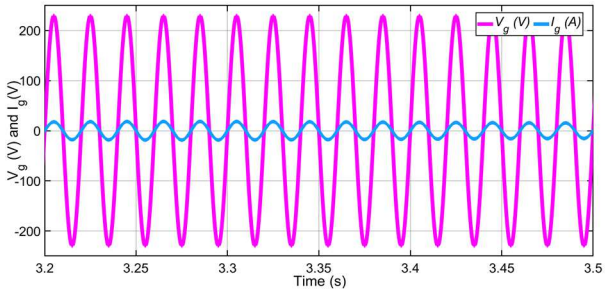

Fig. 7. Grid voltage and current operating at UPF.

C. *Multi-Level Constant Current Charging (MLCC)*

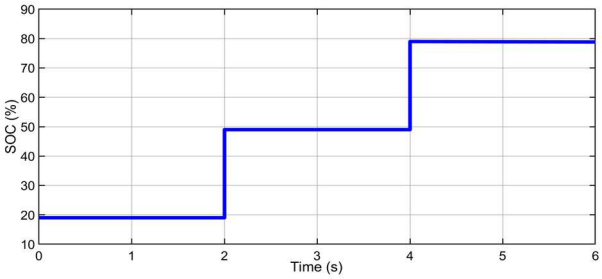

Fig. 8. Step change in SOC of EV battery during MLCC charging.

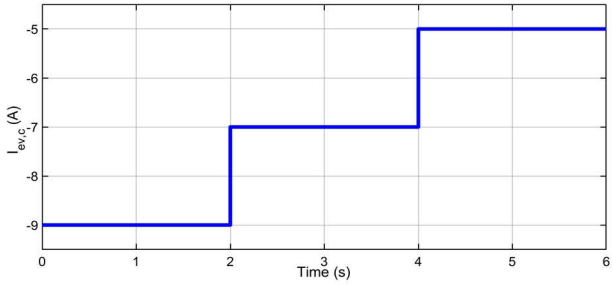

Fig. 9. Step change in EV battery charging current during MLCC method.

As shown in Fig. 8, SOC of the EV battery is changed in a step manner (intentionally) to check the effectiveness of the multi-level constant current method. According to this charging technique, the reference current for charging $(-ve)$ of EV is produced based on SOC of the EV batteries as shown in Fig. 9. In this operating state, the PV power and load demand are constant. Hence, the change in EV charging power is compensated by the utility grid as shown in Fig. 10.

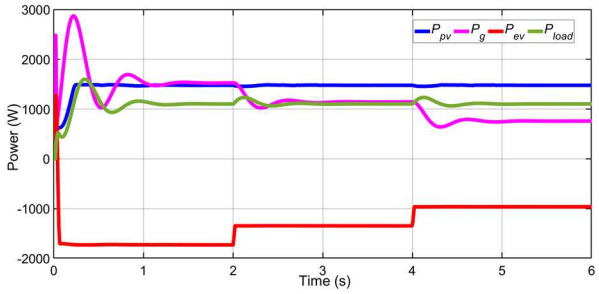

Fig. 10. Different powers of the system during MLCC charging.

D. *Sufficient Power Mode*

During this operation, PV generated power is enough to meet the load requirement and EV charging i.e. $P_{pv} > P_{load} + P_{ev}$. Again the surplus PV power is fed to the connected grid through the DC/AC bi-directional converter. As the extra power is taken by the grid from the microgrid, the grid power is $-ve$ as given in Fig. 11. This condition makes the grid voltage and grid current to be operated at $180°$ phase difference i.e. out of phase operation. The voltage and current plots for the grid are given in Fig. 12.

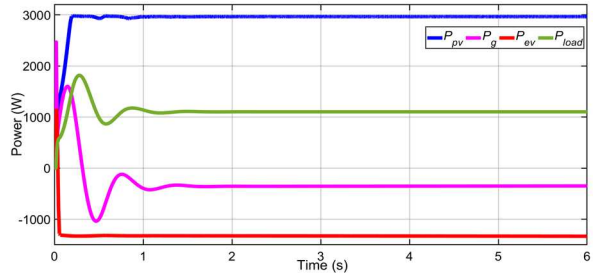

Fig. 11. Different system powers during sufficient power operation.

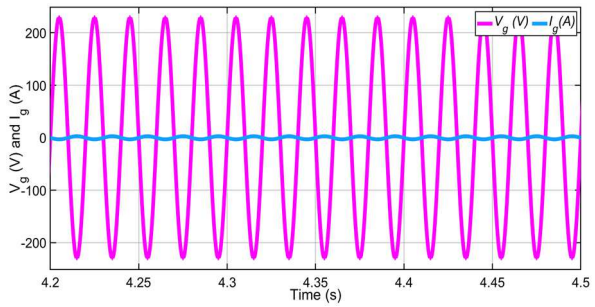

Fig. 12. Grid voltage and current during sufficient power mode.

V. Experimental Results and Discussions

For validation of the designed EV charging station in terms of precise tracking of reference current, smooth transient, and fast dynamics response against sudden disturbances because of generation and load variation in the microgrid system, the experimental results are recorded in real-time in this section. A real-time simulator OP4510 is used for the validation of the proposed control technique, which is portable, compact, and provides high performance, as given in Fig. 13. Fig. 13 shows a complete laboratory set-up with a real-time simulator (OP4510), host system, and digital storage oscilloscope (DSO). The proposed technique is confirmed by the experimental results for the following situations, i)

variation in PV generation, ii) variation in load demand, and iii) MLCC control technique. The main objectives of the explained control technique are to supply uninterruptable power for charging of EV, to maintain a constant voltage of $400V$ at the common DC link, and efficiently maintain the power equilibrium in the system.

Fig. 13. Real-time experimental set-up using OPAL-RT.

A. *Performance during Change of PV Generation*

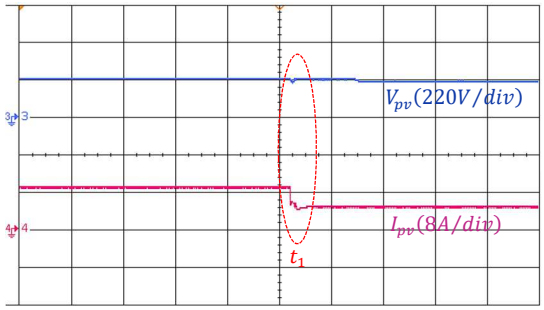

Fig. 14. PV voltage and current for variable generation.

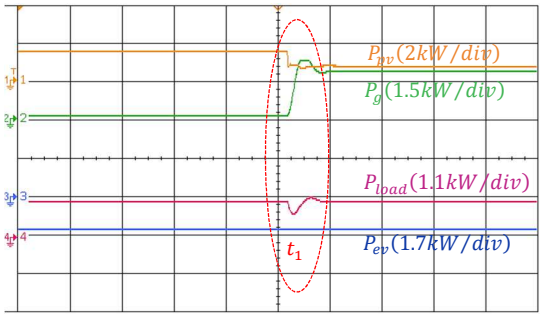

Fig. 15. Experimental result of different power under variable PV generation.

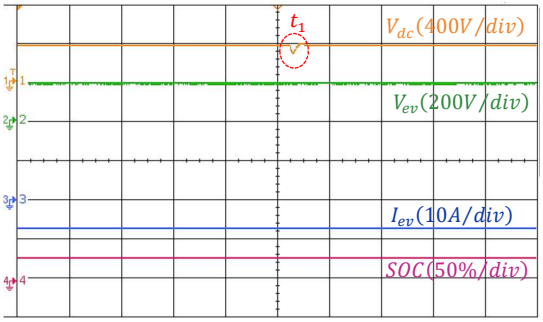

Fig. 16. Experimental result of DC bus voltage and different EV parameters under variable PV generation.

The PV generation is changed by shifting the solar irradiance from $1000\,W/m^2$ to $500\,W/m^2$ at point t_1. The respective change in PV voltage and current are shown in Fig. 14. During this operating condition, EV is charging with constant power and load is also taking constant power from the system. Due to the decrease in PV generation, power supply from the grid is increased at t_1 to fulfill the EV and load power. These power plots are shown in Fig. 15. Irrespective of the change in PV generation, DC bus voltage remains constant as shown in Fig. 16. At the point of generation change, there is an undershoot appeared in the DC bus voltage, but the undershoot is settled within very less time. Respective EV voltage, current, and SOC are also shown in Fig. 16.

B. *Performance during Change of Load Demand*

Here, the system performance is checked for variable loading condition. At point t_1, the load in the system is increased as shown in Fig. 17. As the PV generation is constant during this operation and EV charging power is constant, hence the extra power required by the load is supplied by the utility grid as given in Fig. 17. Because of the load change, there is a voltage undershoot occurred at t_1 in the DC bus voltage as shown in Fig. 18. But within very less time, DC link voltage is recovered to $400V$. The terminal voltage, charging current, and SOC of EV battery are presented in Fig. 18.

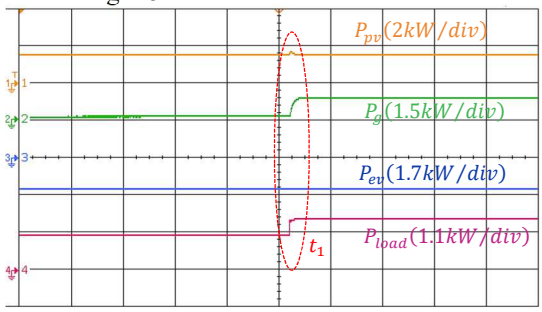

Fig. 17. Different power under changing load condition.

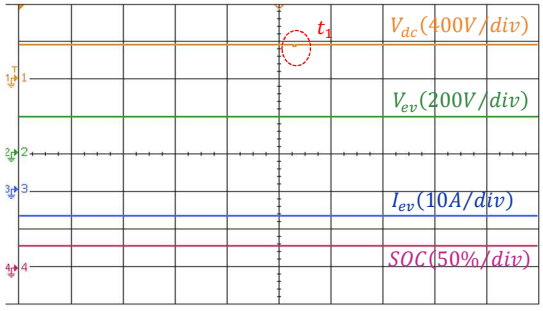

Fig. 18. Experimental result of DC bus voltage and different EV parameters under variable PV generation.

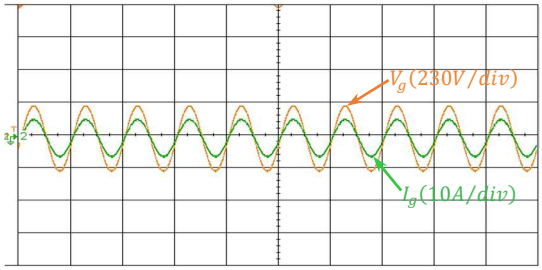

Fig. 19. Grid voltage and current working at UPF.

For a reliable operation of a grid-connected microgrid system, grid voltage and current are required to operate at UPF. This will enhance the power quality features of the microgrid. In the proposed control technique, grid voltage and current are operated at UPF as shown in Fig. 19.

C. Performance in MLCC Method

The control technique used here for charging of EV is the multi-level constant current. To check the efficacy of this technique, the SOC of EV battery is changed intentionally as given in Fig. 20. Initially up to t_1, the EV SOC is less than 20%, hence a charging current of $9A$ is taken by the EV. From t_1 to t_2, the SOC of EV set as 50% and according to the MLCC control, the charging current of EV is decreased to $7A$. Again after t_2, SOC is increased to 75%. Hence, the charging current is decreased to $5A$. All these changes in EV SOC and charging current are shown in Fig. 20. In this paper, the charging current is taken as $-ve$. During these changes the voltage at DC link is retained at $400V$ as presented in Fig. 20. Due to the change in charging current of EV, the power drawn by EV for charging is decreased in step-wise, but the PV and load powers are constant. Hence, to keep the power equilibrium in the EV charging station, the power drawn from the grid is also decreased step-wise as presented in Fig. 21.

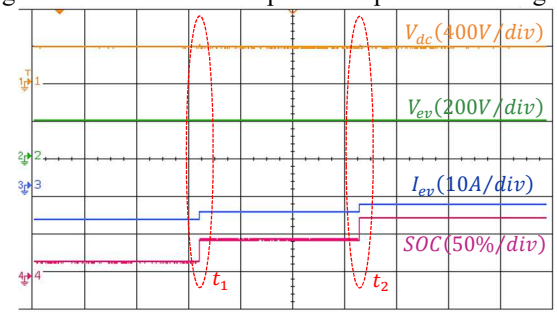

Fig. 20. Experimental result of DC bus voltage and different EV parameters in MLCC method.

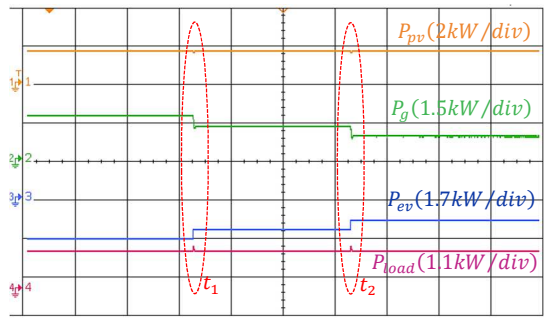

Fig. 21. Different power in MLCC method.

VI. Conclusions

In this paper, an effective multi-level constant current charging method is proposed to evade from overcharging of EV batteries. The PV system is always operated at MPP for optimal utilization of renewable energy. Also, a power equilibrium is maintained irrespective of any changes in the system. By showing both real-time simulation and MATLAB simulation results, the proposed technique is verified. By integrating EV charging with PV microgrids, this system has the potential to contribute to a cleaner and more sustainable transportation system, and also promote the use of renewable energy resources. Further research and implementation of such systems can play a vital role in driving the adoption of EVs and renewable energy technologies, thereby paving the way toward a more sustainable future.

References

[1] M. Yilmaz and P. T. Krein, "Review of Battery Charger Topologies, Charging Power Levels, and Infrastructure for Plug-In Electric and Hybrid Vehicles," *IEEE Transactions on Power Electronics*, vol. 28, no. 5, pp. 2151-2169, May 2013.

[2] P. Goli and W. Shireen, "PV Integrated Smart Charging of PHEVs Based on DC Link Voltage Sensing," *IEEE Transactions on Smart Grid*, vol. 5, no. 3, pp. 1421-1428, May 2014.

[3] A. Verma, B. Singh, A. Chandra, and K. Al-Haddad, "An Implementation of Solar PV Array Based Multifunctional EV Charger," *IEEE Transactions on Industry Applications*, vol. 56, no. 4, pp. 4166-4178, July-Aug. 2020.

[4] V. B. Vu, D. H. Tran, and W. Choi, "Implementation of the Constant Current and Constant Voltage Charge of Inductive Power Transfer Systems With the Double-Sided LCC Compensation Topology for Electric Vehicle Battery Charge Applications," *IEEE Transactions on Power Electronics*, vol. 33, no. 9, pp. 7398-7410, Sept. 2018.

[5] D. van der Meer, G. R. Chandra Mouli, G. Morales-España Mouli, L. R. Elizondo, and P. Bauer, "Energy Management System With PV Power Forecast to Optimally Charge EVs at the Workplace," *IEEE Transactions on Industrial Informatics*, vol. 14, no. 1, pp. 311-320, Jan. 2018.

[6] J. A. D. Navarro, R. D. López, J. M. Y. Loyo, J. S. A. Sevil, and J. L. B. Agustín, "Design of an Electric Vehicle Fast-Charging Station with Integration of Renewable Energy And Storage Systems," *Electrical Power and Energy Systems, Elsevier*, vol. 105, pp. 46-58, Aug. 2018.

[7] D. Steen, L. A. Tuan, O. Carlson, and L. Bertling, "Assessment of Electric Vehicle Charging Scenarios Based on Demographical Data," *IEEE Transactions on Smart Grid*, vol. 3, no. 3, pp. 1457-1468, Sept. 2012.

[8] B. C, S. CK, S. NS, J. Sharma, and J. M. Guerrero, "Interval Type2 Fuzzy Logic-Based Power Sharing Strategy for Hybrid Energy Storage System in Solar Powered Charging Station," *IEEE Transactions on Vehicular Technology*, vol. 70, no. 12, pp. 12450-12461, Dec. 2021.

[9] A. Bharatee, P. K. Ray, and P. S. Puhan, "Power Management in a PV Integrated Electric Vehicle Charging System," *2022 IEEE Global Conference on Computing, Power and Communication Technologies (GlobConPT)*, New Delhi, India, 2022.

[10] B. Singh, D.T. Shahani, and A. K. Verma, "IRPT based control of a 50kW grid interfaced solar photovoltaic power generating system with power quality improvement," *Proceedings of 4th IEEE International Symposium on Power Electronics for Distributed Generation System (PEDG),* Rogers, USA, pp. 1-8, Apr. 2014.

[11] A. Bharatee, P. K. Ray, and A. Ghosh, "A Power Management Scheme for Grid-connected PV Integrated with Hybrid Energy Storage System," *Journal of Modern Power Systems and Clean Energy*, vol. 10, no. 4, pp. 954-963, July 2022.

[12] S. Habib, M. M. Khan, F. Abbas, L. Sang, M. U. Shahid, and H. Tang, "A Comprehensive Study of Implemented International Standards, Technical Challenges, Impacts and Prospects for Electric Vehicles," *IEEE Access*, vol. 6, pp. 13866-13890, 2018.